

# Low-Cost Single-Laser Differential Phase Shift Transmitter Towards SFP-based QKD Tail-End Optics

M. Hentschel, B. Schrenk, R. Lieger, E. Querasser, and H. Hübel

*AIT Austrian Institute of Technology, Dept. Digital Safety & Security, Donau-City Str. 1, 1220 Vienna, Austria.*

*Author e-mail address: michael.hentschel@ait.ac.at*

**Abstract:** A low-cost transmitter based on a single directly-modulated laser is experimentally demonstrated for fibre-based differential phase shift QKD. Chirp modulation is exploited for phase state preparation at 1 GHz symbol rate. A raw key rate of 4.5 kb/s at 2.65% error ratio is obtained after transmission over 27 km. We further demonstrate monolithic integration of pulse carving functionality, leading to a fully-fledged butterfly-packaged QKD transmitter.

## 1. Introduction

Quantum key distribution (QKD) provides the means for establishing a secret key between two communication parties by making use of fundamental laws of quantum mechanics. In most network implementations demonstrated so far [1, 2], individual point-to-point links (with costs incurring several tens of k€) were combined to form a network – without considering capital and operational expenses and consolidation strengths that can mitigate these. By off-loading complexity and head-end equipment associated to high cost to a centralised location, as sketched in Fig. 1(a), tail-end QKD sub-systems can be kept lean and simple, therefore bearing the cost credentials for real-world deployment of QKD services.

In this work we experimentally demonstrate, for the first time to our best knowledge, a low-complexity, GHz-capable differential phase shift (DPS) transmitter based on a single laser, with a form factor promising short-term deployment with small-form factor pluggable (SFP) optics.

## 2. QKD Scheme and Phase State Preparation through Direct Modulation of Laser Gain Section

DPS encodes information in the phase difference between two successive pulses. There is no need for a basis choice, such as, e.g., in the BB84 protocol, hence allowing for a simplistic detection scheme and the utilisation of the full rate of detected photons [3]. In order to facilitate the DPS scheme, cost-effective transmitters are required. Direct phase modulation has been reported previously for semiconductor optical amplifiers [4] and directly modulated lasers [5]. Phase modulation can be exploited in virtue of the chirp property of these semiconductor devices, which introduces transient and adiabatic modulation in the optical phase of a signal. This change in phase  $\Phi$  relates the laser current modulation according to [6]

$$\phi(t) = 2\pi \int \Delta\nu(t)dt = \frac{\alpha}{2} \left[ \ln P(t) + \int \kappa P(t)dt \right]$$

where  $\Delta\nu$  the instantaneous optical frequency change,  $P$  the emitted optical power,  $\alpha$  is the linewidth enhancement factor and  $\kappa$  the adiabatic chirp. Although the parameters  $\alpha$  and  $\kappa$  cannot be directly measured, the interplay of the laser chirp with fibre dispersion does provide information on their magnitude [7]. For example, observing the frequency response dip after transmission over 240 km of standard single-mode fibre with a vector network analyser points to an  $\alpha$  parameter of  $\sim 2.7$  for the directly modulated laser (DML) device under investigation. According to the relation between  $\Phi(t)$  and  $P(t)$  modulation of the laser current with the derivative of the data pattern leads to a non-return-to-zero phase modulation at the laser output, as will be proven shortly. It shall be noted that return-to-zero phase modulation for (optional) pulse carving can be achieved through subsequent intensity modulation. The use of directly modulated semiconductor gain sections has proven to be more efficient than traditional LiNbO<sub>3</sub> modulators when it comes to the driving requirements [4-5,8]. For example, a drive on the order of 1 V<sub>pp</sub> was sufficient to introduce a  $\pi$ -phase shift. Furthermore InP realisations feature small form factors with gain sections in the range of 200 to 400  $\mu\text{m}$ , compared to LiNbO<sub>3</sub> devices requiring a  $\sim 200$ -times larger layout in the cm-range. DML-based solutions and DMLs co-integrated with further modulation sections (such as electro-absorption modulators) are therefore suitable for integration in SFP pluggable optics as commonly used as opto-electronic front-end in communication terminals.

## 3. Experimental Performance Evaluation

The experimental setup is shown in Fig. 1(b). The low-complexity transmitter, located at Bob's premises, comprises a phase modulator to imprint data and a pulse carver to remove transitions in between data

symbols. Two implementations have been evaluated for the transmitter optics, building on a DML used for phase-modulated wavelength emission at  $\lambda_B = 1550.12$  nm with subsequent Mach-Zehnder modulator serving as pulse carver (A in Fig. 1), and a fully-integrated externally modulated laser (EML) comprising of a DML section emitting at  $\lambda_B^* = 1539.6$  nm and an electro-absorption modulator (EAM), packaged in a butterfly module (B). Such transmitter realisations are typically used in SFP+ modules and are mass manufactured, hence, the cost-per-bit for such transmitters has dropped significantly during past years.

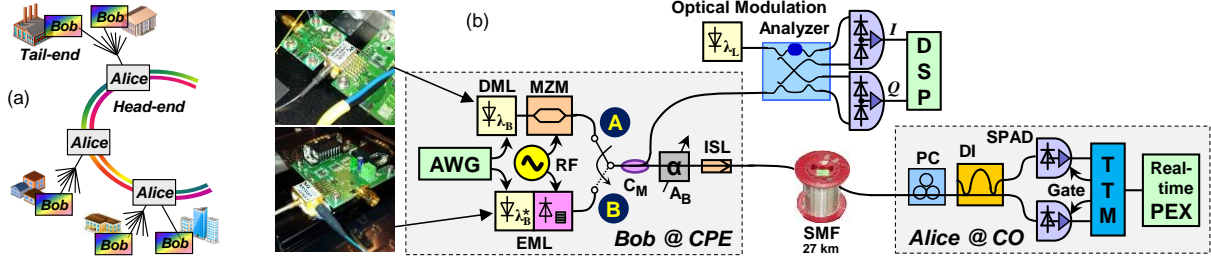


**Fig. 1.** (a) Network context. (b) Experimental setup for DPS-based QKD with low-complexity transmitter at Bob.

Signal generation for phase modulation and pulse carving is performed at 1 Gbaud symbol rate and facilitated through an arbitrary waveform generator (AWG) and a radio frequency (RF) synthesiser, respectively. A pseudo-random bit sequence of length  $2^7-1$  was used for the data symbols. The modulated output is then attenuated ( $A_B$ ), isolated (ISL) and launched with an average photon number  $\mu = 0.1$  per pulse (i.e., symbol) towards the channel. Transmission has been evaluated in a back-to-back configuration and with a 27 km long ITU-T G.652B-compatible standard single-mode fibre (SMF) span.

Receiver opto-electronics with higher degree of complexity are centralised at Alice's point of presence, to which multiple transmitters (Bobs) can connect [3]. A 1-ns delay interferometer (DI) in an asymmetric Mach-Zehnder configuration converts the phase information of the received symbols into intensity modulation after spectral alignment with the spectral response of the DI. A polarisation controller (PC) was used to eliminate residual polarisation-dependency of the DI response. InGaAs single-photon avalanche photo detectors (SPAD) in either output branch of the DI are detecting the demodulated signal at an efficiency of 12.5% and a dead time of 30  $\mu$ s. An external 10 MHz gate with a width of 3.2 ns has been applied. The detection events are registered by a time-tagging module and processed in real-time (PEX) to evaluate raw key rate and error ratio.

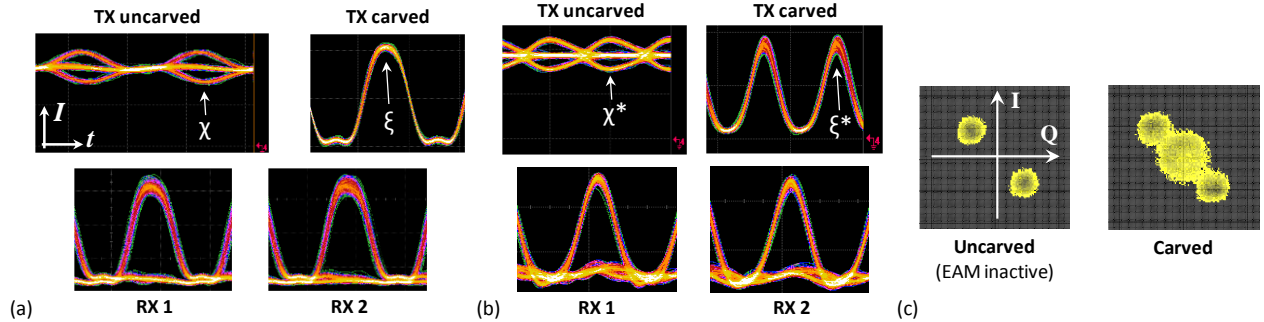


**Fig. 2.** Eye diagrams after transmitter (TX) and receiver (RX) for (a) DML+MZM and (b) EML. Eye diagrams after the transmitter are shown in absence and presence of carving, while receiver eyes are shown for present carving. (c) Constellations in I/Q phase space retrieved by modulation analyser for EML-based transmitter. The carved constellation has been sampled at twice the modulation symbol rate.

#### 4. Signal Generation and Modulation Analysis

The eye diagrams for transmitted and received signals for *DML+MZM configuration* at Bob are presented in Fig. 2(a) and show a superposition of several patterns occurring for the actual data stream over a single symbol period – therefore providing means for signal integrity analysis. While the uncarved DML output resembles a constant-envelope at the centre of the symbol, the modulation transients at the symbol edges ( $\chi$ ) can be suppressed through the pulse carving obtained through the MZM. There is no modulation extinction observed at the centre of the symbol ( $\xi$ ). At the receiver both output branches of the interferometer show a high extinction ratio of more than 12 dB, which evidences the quality of the phase modulation generated through the low-cost transmitter. The RF drive for modulation was  $\sim 10$  mA<sub>pp</sub>.

Figure 2(b) shows the eye diagrams for the *fully-integrated EML-based transmitter*. Similar performance as for the DML+MZM implementation is achieved. The modulation extinction ratio for the pulse carving

introduced by the EAM is 11 dB. However, the reduced electro-optic bandwidth for the laser section of the EML results in wider modulation transitions during phase modulation. This introduces a residual extinction ratio of 0.4 dB at the transmitted signal ( $\xi^*$ ) and reduces the extinction ratio of the received signals after the DI. This limitation is specific for the EML used and not a fundamental impairment.

Inphase/quadrature (I/Q) constellation diagrams have been acquired through optical modulation analysis. Part of the transmitter signal has been split off ( $C_M$ ) and fed to a coherent intradyne receiver based on a  $90^\circ$  hybrid, balanced photo detectors and post-processing using frequency offset estimation to a local oscillator ( $\lambda_L \sim \lambda_B, \lambda_B^*$ ) and a Viterbi-Viterbi  $M^{\text{th}}$ -power phase recovery. The constellations shown in Fig. 2(c) feature a clear  $\pi$ -phase shift between the two modulation symbols and additional signal extinction for the carved transmitter output, for which a state at the origin of the I/Q plane appears in case of sampling at twice the symbol rate.

## 5. Key Rate and Error Ratio

*Transmitter based on DML+MZM:* The raw key rate and error ratio obtained for DML+MZM are presented for back-to-back (Fig. 3(a)) and transmission over SMF (Fig. 3(b)), respectively. The average error ratio obtained is 2.65%. As shown this value remains stable over a longer time span of more than 1 hour, which validates the reliability of the low-cost transmitter. The raw key rates for back-to-back and SMF-based transmission were 18.9 and 4.5 kb/s, respectively. According to theoretical calculations [9] we estimate a fraction of 34% secure key to remain after error correction and privacy amplification.

*Transmitter based on integrated EML:* In case of the EML comparison with the DML+MZM transmitter in terms of raw key rate and error ratio is made for the back-to-back case (Fig. 3(c)). While the raw key rate is similar, the error ratio is increased to 3.8%. This is explained by the aforementioned artefacts arising from the limitation in the electro-optic bandwidth for phase modulation.

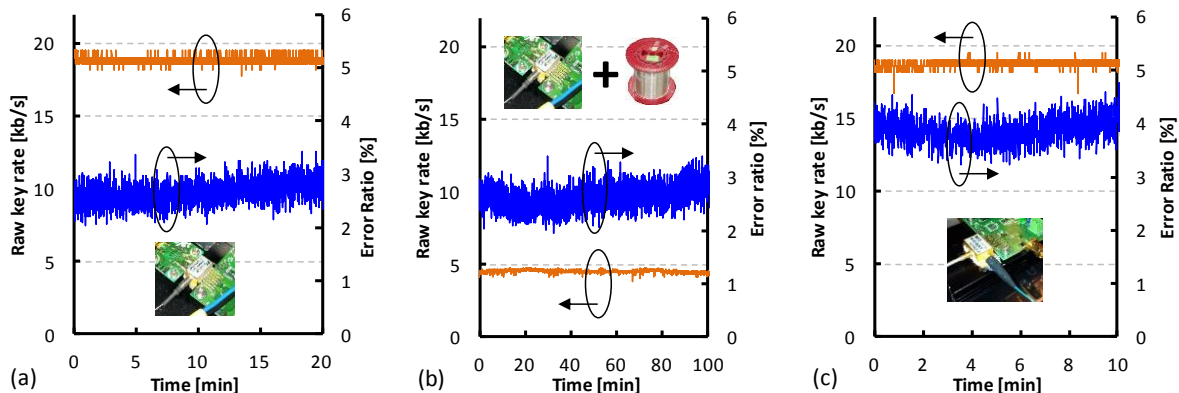


**Fig. 3.** QBER (blue) and raw key rate (orange) for (a) DML+MZM and back-to-back transmission and (b) over 27 km SMF fibre span, (c) integrated EML and back-to-back transmission.

## 6. Conclusions

A low-complexity QKD transmitter for fibre-based networks has been experimentally demonstrated. DML and EML implementations have been evaluated for phase modulation and pulse carving, showing a key rate of 4.5 kb/s at an error ratio of 2.65% after 27 km transmission. The provision of all transmitter functionalities in a single butterfly package poses a leap towards QKD optics with SFP form factor.

## 7. References

- [1] M. Peev et al., “The SECOQC quantum key distribution network in Vienna”, *New J. Phys.* **11**, 075001 (2009).
- [2] M. Sasaki et al., “Field test of quantum key distribution in the Tokyo QKD network”, *Opt. Expr.* **19**, 10387 (2011).
- [3] M. Hentschel et al., “A Differential Phase-Shift Scheme for QKD in Multi-user Telecom Networks”, *Proc. CLEO Europe, Munich, EB-P.4*, 2015.
- [4] B. Schrenk et al., “Flexible quadrature amplitude modulation with semiconductor optical amplifier and electroabsorption modulator”, *Opt. Lett.* **37**, 3222 (2012).
- [5] J. Altabas et al., “Chirp-based direct phase modulation of VCSELs for cost-effective transceivers”, *Opt. Lett.* **42**, 583 (2017)
- [6] R. Tucker, “High-speed modulation of semiconductor lasers”, *Trans. Electron. Devices* **32**, 2572 (1985).
- [7] F. Devaux et al., “Simple Measurement of Fiber Dispersion and of Chirp Parameter of Intensity Modulated Light Emitter”, *J. Lightwave Technol.* **11**, 1937 (1993).
- [8] Z. Yuan et al., “Directly Phase-Modulated Light Source”, *Phys. Rev. X* **6**, 031044, 2016.
- [9] E. Waks et al., “Security of Differential-Phase Shift Quantum Key Distribution against Individual Attacks”, *Phys. Rev. A*, **73** 012344, (2006).